Physica Scripta. Vol. T110, 286–291, 2004

Intense Ultra Slow $\overline{p}$ Beam and its Application

Yasunori Yamazaki[1,2,*]

[1] Graduate School of Arts and Sciences, University of Tokyo, 3-8-1 Komaba, Meguro, Tokyo 153-8902, Japan
[2] Atomic Physics Laboratory, RIKEN, 2-1 Hirosawa, Wako, Saitama 351-0198, Japan

Received September 7, 2003; accepted December 9, 2003

PACS ref: 36.10.−k 39.90.+d 52.27.Jt

Abstract

In the ASACUSA (Atomic Spectroscopy And Collisions Using Slow Antiprotons) collaboration, the Trap group has been working on an efficient accumulation of antiprotons and production of ultra slow mono-energetic antiproton beam, which is realized by a combination of an RFQD (Radio Frequency Quadrupole Decelerator) and a large multi-ring trap (MRT) installed in a super-conducting solenoid. We have succeeded to accumulate several million antiprotons. A mono-energetic antiproton beam of 10 eV has been extracted and transported through a specially designed beam line, which has a high transport efficiency and at the same time enabling differential pumping of more than six orders of magnitude between the MRT and a collision chamber. This configuration was adopted to make atomic collision experiments like ionization and antiprotonic atom formation processes and also to study spectroscopic nature of various meta-stable antiprotonic atoms under single collision conditions, which has never been possible. A new scheme of efficient positron accumulation has been invented employing high-density electron plasma and an ion cloud, which fits quite well with the UHV requirements of antihydrogen synthesis as well as other applications. A so-called cusp trap configuration has been proposed as a new synthesizer of antihydrogen, where antiprotons and positrons can co-exist in the same place even at low temperature. Because of the inhomogeneous magnetic field distribution of the cusp trap, (1) a low energy component of the antihydrogen atom so formed can be trapped for a macroscopic time, and (2) a high energy component emerges as an intensity-enhanced and energy-filtered spin polarized antihydrogen beam, which is suitable for measurements of the hyperfine splitting of antihydrogen, and could provide the magnetic moment of antiproton with some ppm accuracy.

1. Introduction

Atomic physics with slow exotic particles like antiprotons, positrons, muons, and short-lived nuclei are quite interesting providing unique information in various fields of science from basic physics like the CPT (charge, parity, time) symmetry test to applied science like material characterization. However, the fields where they are actively used are rather limited, primarily because these exotic particles are produced in a high-energy region occupying a large phase space volume, and are quite difficult to compress. Further, in the case of antiparticles, the phase space reduction should be done avoiding annihilation with matter. Because of these constraints, all the procedures like cooling, deceleration and accumulation should be done in (ultra high) vacuum. We have been developing new and efficient techniques to accumulate a large number of antiprotons, positrons, and short-lived nuclei, which will be shortly discussed in this report.

The Antiproton Decelerator (AD) at CERN [1] devoted primarily to atomic physics experiments has been stably operated since year 2000 providing 100 MeV/c (5.3 MeV/u) antiprotons of 2×10^7 $\overline{p}s$/pulse every 100 s. With the advent of AD and the progress of experimental programs proposed to utilize antiprotons [2–6], research with slow antiproton beams can now be done much more readily. ASACUSA collaboration (Atomic Spectroscopy And Collisions Using Slow Antiprotons) was formed aiming at studying the nature of antiprotonic helium as well as at developing intense ultra-slow antiproton beams to open new fields of antiproton science including antiprotonic atom formation and antihydrogen synthesis, where atomic physics communities can play essential roles. This report discusses the latter half of the ASACUSA project together with new progress regarding $\overline{H}$ synthesis. Two other proposals have also been approved from the start of AD, the subjects of which are on the production and spectroscopy of antihydrogen. These two groups have recently succeeded in synthesizing antihydrogen atoms ($\overline{H}$) [7,8]. A fourth proposal aiming at applying antiprotons to cancer therapy has newly been approved [27].

One of the most important tools of ASACUSA is the RFQD (Radio Frequency Quadrupole Decelerator) [9], an energy variable decelerator that can provide antiprotons of 10–130 keV with high deceleration efficiency. Slow antiprotons from the RFQD have readily been used for $\overline{p}$He laser spectroscopy in a low pressure He target as well for trapping and extracting ultra-slow antiprotons. Combined with a multiring trap (MRT) [10], several millions of antiprotons are successfully stored and cooled [11,12]. These developments are expected to accelerate not only the elucidation of the process by which antiprotonic atoms are formed, but also the synthesis and study of antihydrogen atoms, and spectroscopic study of antiprotonic atoms like $\overline{p}He^+$ [13].

A conceptually new scheme of antihydrogen synthesis with a mixing trap in a cusp magnetic field is presented [14] together with a UHV compatible scheme of efficient positron accumulation.

2. Purpose

Once a large number of antiprotons ($\overline{p}s$) are stored and ultra slow antiproton beams are prepared, the following research subjects become accessible, which have not been possible at all or have been difficult;

1. Matter–Antimatter symmetry via H and $\overline{H}$ spectroscopy of 1S-2S transitions and hyperfine transitions.
2. Atomic processes with "heavy" electron(s) – elementary processes of ionization and antiprotonic atom ($\overline{p}A^+$) formation.

* e-mail: Yasunori@phys.c.u-tokyo.ac.jp

3. Spectroscopic study of $\overline{p}A^+$ like $\overline{p}p$ in meta-stable states, which has only been possible for $\overline{p}He^+$ because of their extreme meta-stability even in liquid He.
4. Probing nuclear structure of short-lived radio isotope (RI) ions via momentum spectroscopy of residual nuclei after antiproton induced one nucleon pick up.
5. Interaction with solid (surface), elemental analysis, and radiation damage.
6. Non-neutral plasma physics of antiparticles.

Table I shows the present status of the matter-antimatter (a)symmetry with respect to the mass, charge, and *g*-factor for three particle-antiparticle pairs, e^-/e^+, $p/\overline{p}$, and $n/\overline{n}$ [15]. It is seen that the mass and charge difference of these particles have been proved to be the same with a precision of parts in 10^8 (actually the charge to mass ratio q/m is known in parts in 10^{11} by measuring the cyclotron frequency in a Penning trap [16]). The magnetic moment of the antiproton on the other hand, is known only with the precision of parts in 10^3 although that of the proton has been determined down to parts in 10^9 [17]. It is therefore quite important and interesting to determine the antiproton magnetic moment with better accuracy, which could be a potential candidate for high-precision CPT-symmetry tests [18] complimenting 1S-2S laser spectroscopy of antihydrogen. For laser spectroscopy of antihydrogen with the same precision as that of hydrogen (down to parts in 10^{14} [19]), preparation of an intense cold $\overline{H}$ beam or laser cooled $\overline{H}$ atoms is necessary. Antihydrogen atoms in a magnetic bottle could be another possibility at the cost of resolution due to its magnetic field inhomogeneity. It is noted that the magnetic bottle does not coexist with a nested trap with a uniform magnetic field, which has been commonly used in antihydrogen synthesis. The key issue is then to invent a proper scheme to prepare an ensemble of "high quality" antihydrogen suitable for experiments. A possible candidate is discussed in Section 4.

Item 2, atomic physics with a "heavy" electron, was discussed previously [11] and is not repeated here. It is noted that a full quantum mechanical calculation of protonium formation has recently been reported [20]. High precision laser spectroscopy of meta-stable $\overline{p}He^+$ has a long history and has been intensively studied by the ASACUSA collaboration, as has recently been summarized in a review article [13]. One of the interesting applications of $\overline{p}A$ is to probe the neutron and proton distribution [21]. Once an antiprotonic atom is formed with an antiproton in a high Rydberg state ($n \sim 40$), it cascades down emitting Auger electrons and X rays, and eventually annihilates with a proton/neutron near the surface of the nucleus. It is then expected that an analysis of the residual nuclei provides the spatial and momentum distributions of protons and neutrons near the surface of the nucleus. Such an investigation could be applied to short-lived nuclei [22]. We have developed a so-called RF Ion Guide technique [23] to produce thermal RI ions, which allow to study, e.g., the Bohr–Weisskopf effect [24] via high-resolution laser and microwave spectroscopy, the mass formula of short-lived RI, etc. RI ions are supplied from a projectile fragment separator with much less restriction on the chemical and material properties and lifetimes, which is quite different from the ISOL (Isotope Separator On-Line) scheme [25]. The recombination process between an antiproton and an ion has been theoretically studied, which predicts that the recombination cross sections could be comparable to or even larger than neutral targets [26]. The item 5 has practical importance, e.g., in constructing high sensitive detectors for slow antiprotons, and also in cancer therapy with antiprotons [27].

Table I. *A couple of examples of particle and antiparticle symmetry Ref. [15].*

	$(m_m - m_a)/m$	$(q_m - q_a)/q$	$(g_m - g_a)/g$
e^- vs e^+	$< 8 \times 10^{-9}$	$< 4 \times 10^{-8}$	$(-0.5 \pm 2.1) \times 10^{-12}$
p vs$\bar{p}$	$(-2 \pm 2.3) \times 10^{-8}$	$(-2.5 \pm 2.3) \times 10^{-8}$	$(-2.6 \pm 2.9) \times 10^{-3}$
n vs$\bar{n}$	$(9 \pm 5) \times 10^{-5}$	—	—

3. $\overline{p}$ Accumulation

Antiprotons are produced in proton-nucleon collisions, e.g.,

$$p + p \rightarrow \overline{p} + p + p + p.$$

The threshold kinetic energy of a proton to produce an antiproton is ~ 6 GeV, and the corresponding minimum kinetic energy of the antiproton in the laboratory frame is ~ 1 GeV. In the case of AD which is schematically shown in Fig. 1, 3.5 GeV/c antiprotons produced with 26 GeV/c protons are accumulated, cooled, and decelerated down to 100 MeV/c (5.3 MeV/u), and are eventually extracted as a pulsed beam of 90 ns in width containing 2×10^7 antiprotons every ~ 100 s. Usually, a simple degrader foil technique is applied to this 5 MeV beam to prepare antiprotons around 10 keV and lower for trapping. In this case, the trapping efficiency cannot be great at all, because the energy spread after large energy loss is quite large, actually much larger than the resultant average energy [28], and a considerable fraction of antiprotons are stopped and annihilate in the degrader foil. In order to overcome this bottle-neck difficulty, an RFQD (Radio Frequency Quadrupole Decelerator) [29], an energy variable decelerator (10–130 keV), has been installed in the ASACUSA beamline as shown in Fig. 1. The deceleration efficiency has been found to be $\sim 25\%$, i.e., ~ 5 million antiprotons are supplied from the RFQD per one AD shot. Antiprotons so decelerated are injected in an MRT (MultiRing Trap) [10] via two thin foils ($\sim 90\,\mu g/cm^2$ each), which "decelerate" antiprotons with energies less than 10 keV and also isolate the trap vacuum from the RFQD vacuum. Decelerated antiprotons are reflected by a downstream end electrode of the MRT, which is biased at -10 kV. Before the reflected antiprotons reach an upstream end electrode, which is grounded when the decelerated antiprotons are coming in is now biased at -10 kV with a fast switch, thus antiprotons are confined in the MRT. Antiprotons are then cooled below eV with electrons preloaded at the center of the MRT, and eventually condense together with electrons. At the moment, ~ 1 million antiprotons are stored per one AD shot, which is several tens times more efficient than the simple degrader foil scheme. By stacking antiprotons for several AD shots,

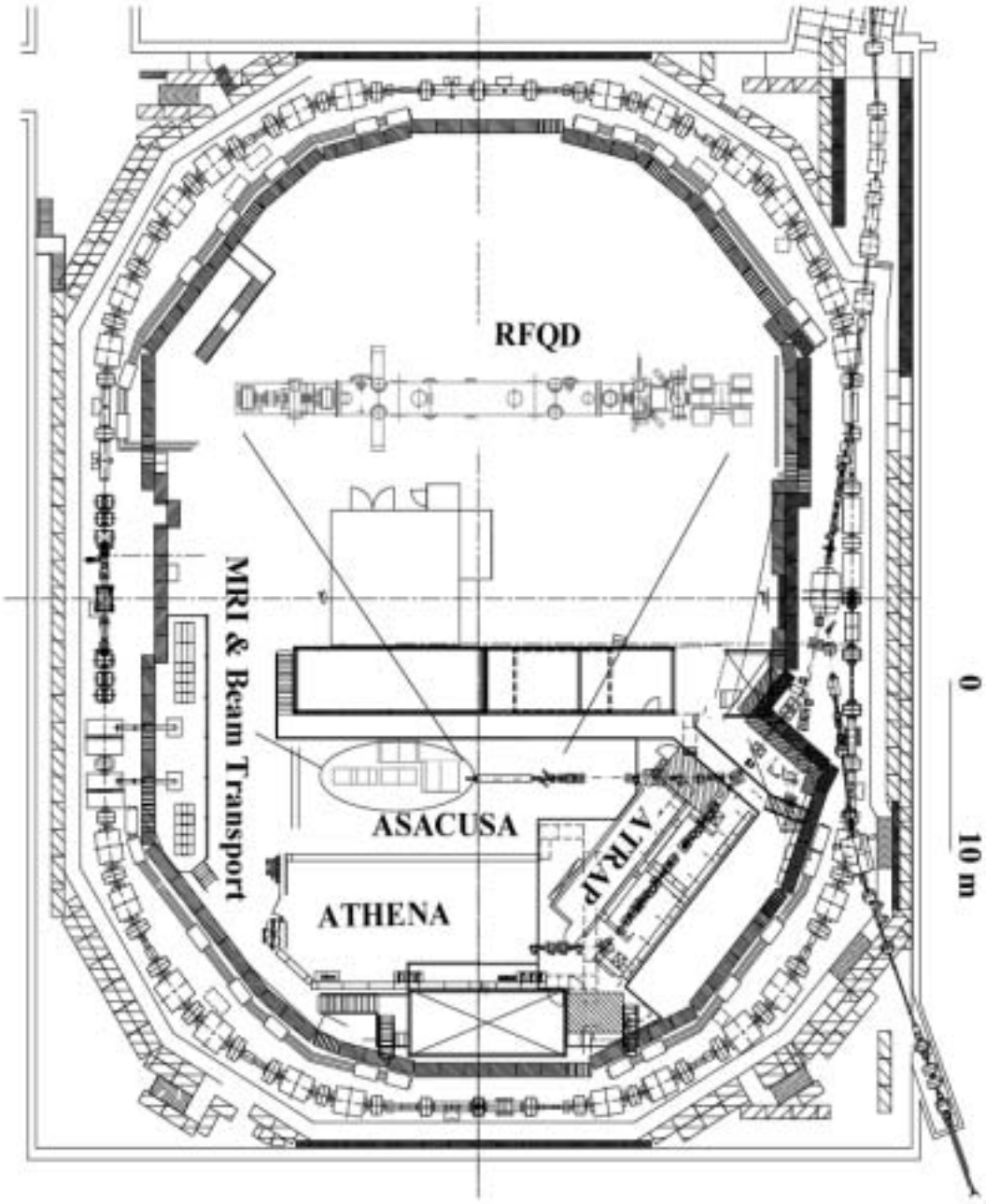

Fig. 1. A schematic layout of AD, ASACUSA, ATHENA, and ATRAP. A magnified view of the RFQD is shown in the left half of AD.

several million antiprotons are accumulated, which is the largest number ever stored at rest. By this way, the energy of the antiprotons is reduced more than 9 orders of magnitude. The electrodes around the center of the MRT are biased so that a harmonic potential is formed along the trap axis, which enables stable trapping of a large number of antiprotons [10], and at the same time to figure out the shape, density, and temperature of the electron plasma non-destructively by monitoring electrostatic eigenmodes of the plasma. For example, the frequency evolution of the (2,0) and (3,0) modes have been successfully observed when antiprotons are injected, revealing that the plasma temperature rises about 0.6 eV within a few seconds, and then returns slowly to the original temperature in a few tens seconds [30]. A similar feature has also been observed for proton cooling with electrons [31].

Cold antiprotons are then extracted as an ultra-slow mono-energetic beam of 10 eV–500 eV through a specially designed beam line [32], which enables to transport antiprotons with high efficiency at the same time realizing a large differential pumping ability of more than 6 orders of magnitude.

4. Polarized $\overline{\mathrm{H}}$ beam with a cusp trap

The successful trapping of a large number of antiprotons and extraction of them as ultra-slow $\overline{\mathrm{p}}$ beams will accelerate not only the elucidation of the process by which antiprotonic atoms are formed, but also the synthesis and study of antihydrogen atoms. According to this line, a new scheme of cold antihydrogen synthesis has been proposed [14], where a recombination trap consisting of a magnetic quadrupole (cusp) formed by a pair of superconducting solenoids (see Fig. 2) and an electrostatic octupole formed by five axially-symmetric electrodes is used, which is referred to as an MCEO (magnetic cusp and

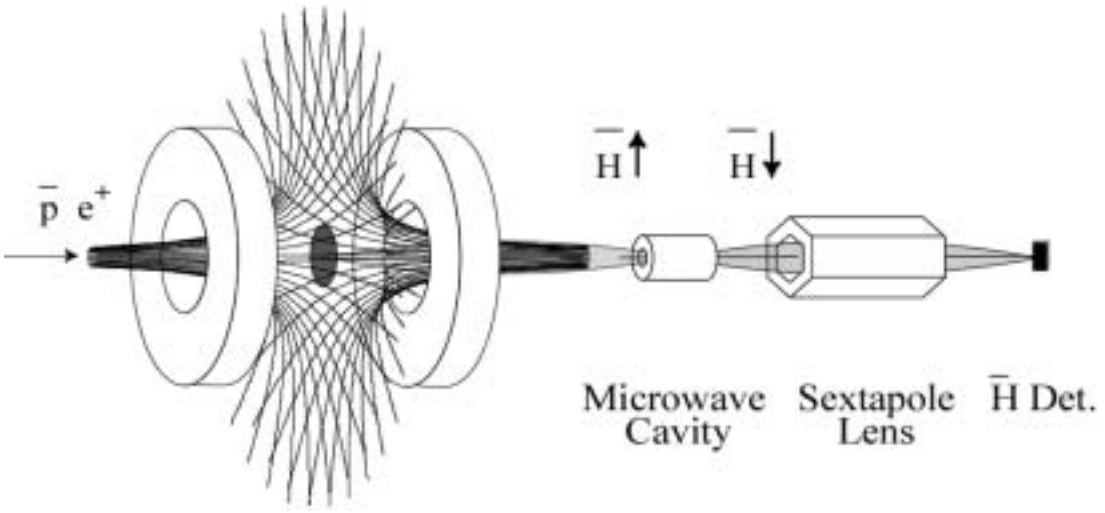

Fig. 2. A schematic layout of the cusp trap configuration (the left half) together with a microwave cavity and a magnetic sextupole lens for hyperfine transition measurements.

an electric octupole) trap hereafter. Slow positrons injected in the MCEO oscillate along the magnetic field line if the octupole electric field is applied after the injection [34]. Figure 3 shows the electric potential distribution by contour lines. In an inhomogeneous magnetic field $\boldsymbol{B}$, a positron with the orbital magnetic moment μ_c is subject to the force $-|\mu_c|\nabla|\boldsymbol{B}|$. In other words, positrons are in equilibrium along the magnetic field direction when the force due to their space charge balances with the sum of the octupole electric field and $-|\mu_c|\nabla|\boldsymbol{B}|$, i.e., some excess positrons can be stored in the MCEO [35]. The maximum magnetic field of the MCEO is designed to be $\sim$3.5 T with a field gradient as strong as $\sim$30 T/m, i.e., positrons are cooled down via synchrotron radiation to the environmental temperature of $\sim$4 K. After positrons are stored and cooled, antiprotons are introduced along the MCEO axis. An additional electric field is necessary to confine antiprotons until they are thermalized, which is realized by a couple of electrodes covering the MCEO from outside as shown in Fig. 3. An example of the simulated antiproton trajectories is plotted in Fig. 3, indicating its stability. Because of the excess charge of positrons discussed above, antiprotons will condensate at the center of the MCEO once they are cooled down, forming an electrically neutral mixture of positrons and antiprotons in the central part. As a natural consequence, efficient antihydrogen synthesis will take place even at very low temperature. This feature is quite different from the nested trap scheme.

An antihydrogen formed at the center of the MCEO drifts into an area where the magnetic field is finite, where an $\overline{\mathrm{H}}$ atom with total spin $F = 1$ splits into three states, $(F, M_F) = (1, 1), (1, 0), (1, -1)$ according to the total magnetic quantum number M_F. The magnetic moment μ_c in the state (1,1) or (1,0) is anti-parallel to the magnetic field $\boldsymbol{B}$ and such states prefer lower fields (LS: low-field seeker states) while the $(1, -1)$ state and the (0,0) state ($F = 0$) move towards higher fields (HS: high-field seeker states). LS atoms are decelerated when they move outward and deflected if their kinetic energies are lower than the potential barrier of the cusp magnetic field ($\sim$0.2 meV), i.e., the MCEO acts as an $\overline{\mathrm{H}}$ trap. However, when their energy is higher than the potential barrier, they are focused like in the case of an electrostatic charged particle lens.

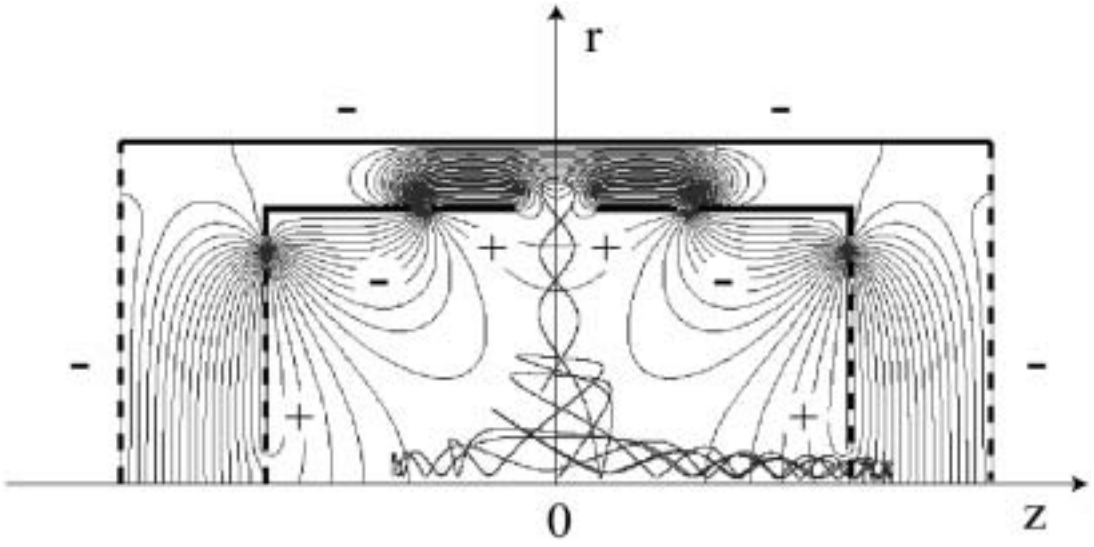

Fig. 3. Electrode configuration for the octapole electric field formation for positron trapping and the outer electrodes for hot antiproton confinement (symmetric with respect to the axis z). The solid lines show the equi-potential lines in and outside the MECO. An example of the trajectories of 30 eV antiprotons is also given.

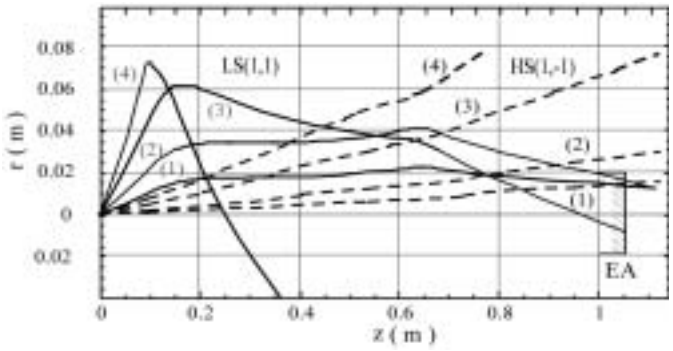

Fig. 4. The solid lines are the trajectories of 0.268 meV Hs in the LS(1,1) state with emission angles $q = (1)5$, (2) 10, (3) 20, and (4) 30°. The dotted lines are those of 0.268 meV Hs in the HS(1, −1) state with the emission angle $q = (1)$ 0.5, (2) 1.1, (3) 3, and (4) 5°. The EA indicates the entrance aperture of the microwave cavity.

The solid lines in Fig. 4 show trajectories of 0.268 meV $\overline{\mathrm{H}}$ atoms in LS(1,1) states formed at the center of the MCEO. It was found that such LS atoms with divergence angle $\theta < 24°$ can pass the entrance aperture of a microwave cavity (EA in Fig. 4) having a geometric acceptance angle of $\theta \sim 1°$, i.e., the antihydrogen flux reaching the EA is enhanced by two and a half orders of magnitude. On the other hand, HS antihydrogen atoms are defocused and those emitted with $\theta > 0.9°$ do not reach the observation area, i.e., the antihydrogen beam reaching the microwave cavity is more than 99% spin-polarized.

As shown in Fig. 2, the antihydrogen beam in LS states is then spin-flipped in the microwave cavity if the frequency matches, passes through the sextupole lens (magnet) and finally focuses on the $\overline{\mathrm{H}}$ detector if they are in HS states. Technically, this part has been well established with atomic hydrogen experiments sometime ago. Again the key issue is the preparation of a proper antihydrogen beam. Considering that the interaction time of antihydrogen with the microwave field is ~1 ms (a few hundreds of m/s in velocity and a cavity size of a fraction of m, the order of the microwave wavelength), the expected accuracy of the antiproton magnetic moment is of the order of ppm, which is 3 orders of magnitude improvement over the present accuracy (see table I).

$\overline{\mathrm{H}}$s in LS states with relatively low kinetic energies are selectively trapped, i.e., the MCEO is an accumulator/reservoir of spin-polarized antihydrogen atoms, which can supply a pulsed, spin-polarized, low energy antihydrogen beam. The lifetime of the $\overline{\mathrm{H}}$ ensemble in the trap may be determined by the frequency of the Majorana spin-flip transitions [36], which take place only in the $B \sim 0$ region very close to the center of the MCEO, and the practical trapping time is expected to be much longer than a second [37].

5. Positron accumulation

The accumulation of a large number of positrons is, in addition to the $\overline{\mathrm{p}}$ accumulation discussed in Section 3, the key ingredient to synthesize antihydrogen. We have developed an efficient and UHV (ultra high vacuum) compatible accumulation scheme. Once a large number of positrons are stored, a variety of applications emerge, which include low energy atomic collisions [38,39], plasma physics [40], positronium production [41,42], and positron cooling of highly charged ions [43]. Until now, resistive cooling [44] and field ionization of positronium in high Rydberg states [45] have been developed as UHV compatible schemes employing ^{22}Na source although their efficiencies are relatively low (~2.8, and ~11 e^+/s/mCi, respectively). When UHV requirements are relaxed, a N_2 buffer gas method has been proved to be efficient [46], which yields more than 10^4 e^+/s/mCi, where positrons are accumulated in vacuum of 10^{-4} Pa. We discuss here a new positron accumulation scheme, where a combination of high-density electron plasma and an ion cloud is used as "stoppers" of positrons.

Figure 5 shows a schematic configuration of the experimental setup [47], which consists of an electron gun, a multi-ring trap (MRT), a movable W(100) re-moderator, a faraday cup, and a NaI γ-ray detector. The MRT and re-moderator are in a cryogenic UHV bore tube of a 5 T superconducting solenoid. Slow positrons from a solid Ne moderator are transported into the MRT and injected on the re-moderator. Low energy positrons from the re-moderator are accumulated through collisions with high-density electron plasma and an ion cloud in the MRT.

Figure 6 shows the accumulation efficiency of positrons as a function of the number of electrons in the plasma, which increases monotonically and then flats off. It is seen that an accumulation rate as high as 400 e^+/s/mCi is reached, which is more than 30 times higher than other UHV compatible schemes. It was found that the positron accumulation proceeds even without ions although the efficiency is reduced by a factor of 10 (the open circle in Fig. 6) but no positrons are trapped without electrons, i.e., the primary process observed here is the energy loss in the electron plasma and then the momentum transfer collisions with ions in the positron trap.

The maximum trapping efficiency is calculated considering the stopping power of positrons in electron plasma [48], which can more or less reproduce the observed behavior in Fig. 6.

5. Summary & future

New schemes to effectively accumulate a large number of antiprotons and positrons are discussed together with a

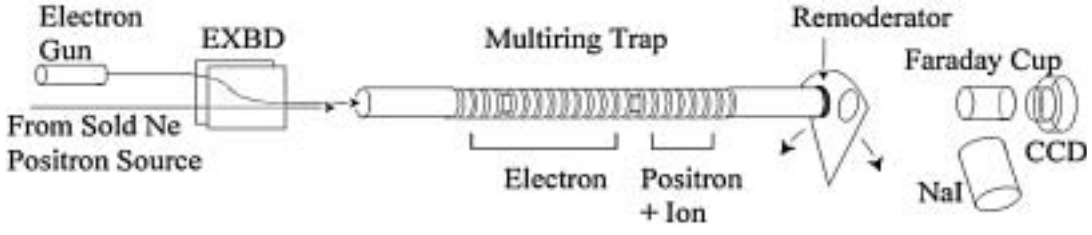

Fig. 5. A schematic diagram of the experimental setup for the UHV compatible positron accumulation (See the text for details). [47]

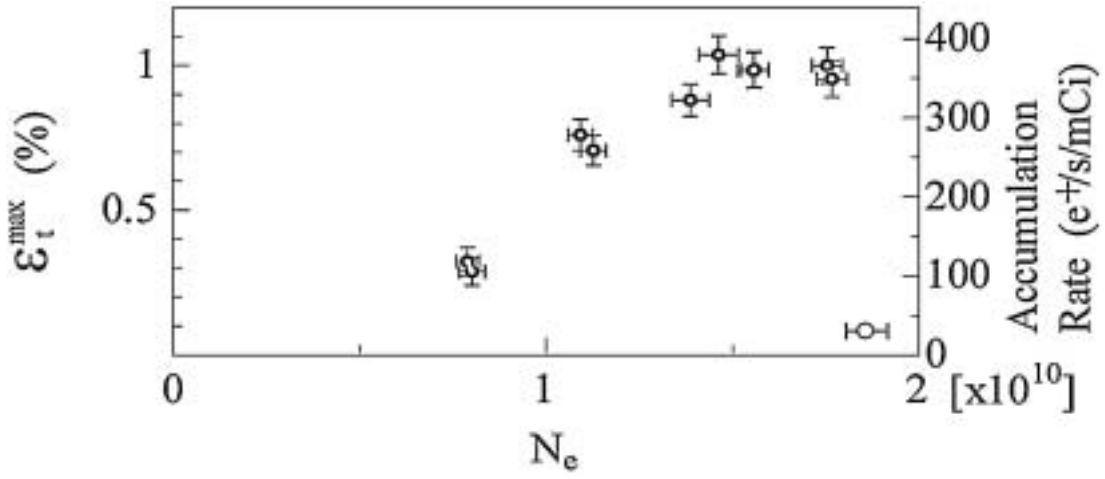

Fig. 6. The optimized trapping efficiency as a function of the total electron number in the electron plasma. The right vertical scale gives the accumulation rate normalized by the ^{22}Na positron source intensity [47].

scheme to prepare intense spin-polarized antihydrogen beams. Whenever some physical quantity (quality) is improved more than an order of magnitude, a new field will start and grow, which is what we are expecting in the field of exotic particles.

At the moment, a 50 GeV proton synchrotron is under construction (Jparc Project) in Japan, and a 90 GeV proton synchrotron has also got a green light to proceed in Germany. The proton energies of both machines are far above the production threshold of $\overline{\mathrm{d}}$ and $\overline{\mathrm{t}}$, antiparticles heavier than $\overline{\mathrm{p}}$, i.e., in principle one can decelerate and store them in a trap and synthesize $\overline{\mathrm{D}}$, $\overline{\mathrm{T}}$, etc. in a foreseeable future.

Acknowledgements

The author is grateful to the AD, RFQD and CERN staffs for their efforts in providing the antiproton beam for the experiment, and is deeply indebted to the collaborators of the ASACUSA project, particularly the members of the ASACUSA Trap group, N. Kuroda, A. Mohri, H. A. Torii, M. Hori, J. Eades, W. Pirkl, H. Higaki, K. Yoshiki Franzen and K. Komaki for their fruitful and vivid discussions. Deep thanks are also due to the RIKEN positron trap group, N. Ohshima, M. Niigaki, T. Kojima and A. Mohri, to the RIKEN cusp trap group, Y. Kanai, A. Mohri and to the RIKEN RF Ion guide group, M. Wada, T. Nakamura and A. Takamine for their excellent ideas and hard work. The author is also happy to thank A. Endo for her elaborate work on the simulation of the antiproton trajectories. The work is supported by a Grant-in-Aid for Creative Basic Science (10NP0101), Ministry of Education, Science, and Culture, and also by Special Research Projects for Basic Science of RIKEN.

References

1. Maury, S., Hyperfine Interactions **109**, 43 (1997).
2. Eades, J. and Hartman, F. J., Rev. Mod. Phys. **71**, 373 (1999).
3. Holtzscheiter, M. H. and Charlton, M., Rep. Prog. Phys. **62**, 1 (1999).
4. Azuma, T. *et al.*, (1997) CERN Proposal SPSC 97-19/P307.
5. Gabrielse, G. *et al.*, (1997) CERN Proposal SPSC 97-8/P306.
6. Holzscheiter, M. H. *et al.*, (1996) CERN Report SPSLC/96-47/P302.
7. Amoretti, M. *et al.*, Nature **419**, 456 (2002).
8. Gabrielse, G. *et al.*, Phys. Rev. Lett. **89**, 213401 (2002).
9. Bosser, J. *et al.*, (1997) CERN Report PS/HP Note 97-36.
10. Mohri, A., *et al.*, Jpn. J. Appl. Phys. **37**, 664 (1998).
11. Yamazaki, Y., Nucl. Instr. Meth. B **154**, 174 (1999), Yamazaki, Y., Hyperfine Interactions **138**, 141 (2001).
12. Kuroda, N. *et al.*, private communication.
13. e.g., Yamazaki, T. *et al.*, Phys. Rep. **366**, 186 (2002).
14. Mohri, A. and Yamazaki, Y., Europhys. Lett. **63**, 207 (2003).
15. Hagiwara, K. *et al.*, Phys. Rev. D **66**, 010001 (2002).
16. Gabrielse, G. *et al.*, Phys. Rev. Lett. **82**, 3198 (1999).
17. Essen, L. *et al.*, Nature **229**, 110 (1971), Winkler, P. F. *et al.*, Phys. Rev. A **5**, 83 (1972).
18. e.g., Kostelecky, V. A., Phys. Rev. Lett. **80**, 1818 (1998).
19. Niering, N. *et al.*, Phys. Rev. Lett. **84**, 5496 (2000).
20. These proceedings and Phys. Rev. A **65**, 012706 (2001).
21. Bugg, W. M., Condo, G. T., Hart, E. L., Cohn, H. O. and McCulloch, R. D., Phys. Rev. Lett. **31**, 475 (1973), Jastrzebski, J. *et al.*, Phys. Rev. C **47**, 216 (1993), Lubinski, P. *et al.*, Phys. Rev. Lett. **73**, 3199 (1994).
22. Wada, M. and Yamazaki, Y., Nucl. Instr. Meth. B **214**, 196 (2004).
23. Wada, M. *et al.*, Nucl. Instr. Meth. B **204**, 570 (2003).
24. Bohr, A. and Weisskopf, V. F., Phys. Rev. **77**, 94 (1950), Wada, M. *et al.*, Hyp. Inter. **81**, 161 (1993).
25. e.g., Huyse, M. *et al.*, Nucl. Instr. Meth. B **187**, 535 (2002).
26. Cohen, J., Phys. Rev. A **69**, 022501, (2004).
27. Maggiore, C. *et al.*, CERN-SPSC-2002-030 proposal (2002).
28. Tschalaer, C., Nucl. Instr. Meth. **64**, 237 (1968).
29. Bylinsky, Y., Lombardi, A. M. and Pirkl, W., CERN-PS-2000-061-PP (2000).
30. Kuroda, N. *et al.*, to be published.
31. Higaki, H. *et al.*, Phys. Rev. E **65**, 046410-1 (2002).
32. Yoshiki Franzen, K. *et al.*, Rev. Sci. Instrum. **74**, 3305 (2003).
33. Tiouririne, T. N., Turner, L. and Lau, A. W., Phys. Rev. Lett. **72**, 1204 (1994).
34. Mohri, A. *et al.*, Jpn. J. Appl. Phys. **37**, L1553 (1998).
35. Mohri, A. *et al.*, Proc. 27th EPS conference on controlled fusion and plasma phys. (ed. Szeoe *et al.*), Vol. **24B**, (2000), pp. 149.
36. Majorana, E., Nuovo Cimento **9**, 43 (1932).
37. Migdall, A. L. *et al.*, Phys. Rev. Lett. **54**, 2596 (1985).
38. Gilbert, S. *et al.*, Phys. Rev. Lett. **82**, 5032 (1999).
39. Walker, A. B. *et al.*, Phy. Rev. B **46**, 1687 (1992).
40. Greaves, R. G. and Surko, C. M., Phys. Rev. Lett. **75**, 3846 (1995); Greaves, R. G. and Surko, C. M., Phys. Rev. Lett. **85**, 1883 (2000); Jelenkovic', B. M. *et al.*, Nucl. Instr. Meth. B **192**, 117 (2002).
41. Chu, S. and Mills, Jr., A. P., Phys. Rev. Lett. **48**, 1333 (1982).
42. Mills, Jr., A. P., Nucl. Instr. Meth. Phys. Res. B **192**, 107 (2002).
43. Mohri, A. *et al.*, "Non-Neutral Plasma Physics IV" (Melville, New York, 2002) (Edited by F. Anderegg, *et al.*), AIP CP606, p. 634; Kanai, Y. *et al.*, Physica Scripta **T92**, 476 (2001).
44. Haarsma, L. H. *et al.*, Phys. Rev. Lett. **75**, 806 (1995).
45. Estrada, J. *et al.*, Phys. Rev. Lett. **84**, 859 (2000).
46. Surko, C. M. *et al.*, Phys. Rev. Lett. **62**, 901 (1989); Greaves, R. G. *et al.*, Phys. Plasmas **1**, 1439 (1994).
47. Ohshima, N. *et al.*, private communication.
48. Sivukhim, D. V., Rev. Plasma Physics Vol. **4**, (Edited by M. A. Leonitovitch), (Consultant Bureau, New York, 1966), p. 93.
49. http://j-parc.jp/Acc/50GeV/50GeV.top.html
50. http://www.gsi.de/GSI-Future/cdr/

